Letters

Alternate Arm Converter Energy Balancing Under Parameter Variation

Harith R. Wickramasinghe, *Member, IEEE*, Georgios Konstantinou, *Senior Member, IEEE*, Salvador Ceballos, and Josep Pou, *Fellow, IEEE*

***Abstract*—Energy balancing of the alternate arm converter (AAC) is a major challenge and overlap period-based circulating current control methods are commonly used. Component parameter variation occurs due to tolerances, component aging, and internal faults leading to stored energy imbalances of modular voltage source converter (VSC) topologies. If not controlled, such variations can severely impact the operation of the AAC. Hence, component parameter variation is a key consideration for energy balancing of all sorts of modular VSC topologies, but has not been addressed in the existing literature for the AAC. This paper investigates the energy balancing capability of the AAC in high-voltage direct current (HVDC) applications under component parameter variations and proposes a compensation method to further improve its energy balancing performance. The effectiveness of the proposed method is verified in a real-time model of an AAC-HVDC transmission system from widely accepted existing CIGRE benchmark models.**

***Index Terms*—Alternate arm converter (AAC), energy balancing, high-voltage direct current (HVDC), parameter variation.**

I. Introduction

APPLICATIONS of modular voltage source converter (VSC)-based high-voltage direct current (HVDC) systems [1] are increasing in modern power systems owing to their unique features over conventional VSCs and line-commutated current source converters [2]. The alternate arm converter (AAC) [3] is an emerging dc fault-tolerant topology combining characteristics of the MMC and two-level converter in a modular VSC topology. Despite the need for a dc-link capacitor, the total stored energy remains lower than other equivalent topologies [4]. Due to the topology and operation of the AAC, the inherent energy balancing is confined to one operating point called the "sweet-spot" [3] that belongs to the overmodulation

Manuscript received July 3, 2018; revised July 31, 2018; accepted August 14, 2018. Date of publication August 26, 2018; date of current version February 20, 2019. This work was supported under Australian Research Council's Discovery Early Career Research Award (DECRA-DE170100370). *(Corresponding author: Harith R. Wickramasinghe.)*

H. R. Wickramasinghe and G. Konstantinou are with the School of Electrical Engineering and Telecommunications, UNSW Sydney, Sydney, NSW 2052, Australia (e-mail:

the SM capacitor energy. Therefore, the stored energy depends on the operating point. Inherent energy balancing is achieved only when the net exchanged energy of an arm is zero over each half-cycle [3] and the operating point is called the "sweet-spot" ($m_a = 4/\pi$). Conventionally, a small duration ("overlap period") around the zero-crossing points of v_a is provided by overlapping the operation of DSs, allowing a common circulating current to balance the stored energy of the phase-leg at nonsweet-spot operation.

III. Energy Balancing Under Parameter Variation

A. AAC Operation Under Arm Inductor Variation

Considering the alternate operation of the arms, the output voltages for the positive and negative half-cycles can be written as

$$v_a = \frac{V_{\rm dc}}{2} - d_u N V_C - L\frac{di_a}{dt}, \quad \text{and} \tag{1}$$

$$v_a = -\frac{V_{\rm dc}}{2} + d_l N V_C - L\frac{di_a}{dt} \tag{2}$$

respectively, where d_u and d_l are the duty cycles of the arms. Considering arm inductance variations (ε_{Lu} and ε_{Ll}) and the resultant SM capacitor voltage deviation (δV_C), the output voltage of (1) and (2) can be expressed as

$$v_a = \frac{V_{\rm dc}}{2} - d_u N(V_C + \delta V_C) - (1-\varepsilon_{Lu})L\frac{di_a}{dt}, \quad \text{and} \tag{3}$$

$$v_a = -\frac{V_{\rm dc}}{2} + d_l N(V_C - \delta V_C) - (1-\varepsilon_{Ll})L\frac{di_a}{dt}. \tag{4}$$

Assuming a strong ac grid and that the power flow to the ac grid remains unchanged, the variation of v_a is negligible. Hence, the terms $\varepsilon_{Lu}L\frac{di_a}{dt}$ and $\varepsilon_{Ll}L\frac{di_a}{dt}$ of (3) and (4) are compensated by the arm duty cycles (d_u and d_l) in order to maintain v_a similar to the balanced conditions. Consequently, stored energy of the arms deviate due to the variation of the duty cycles. The SM capacitor voltage deviations of the two arms are opposite and equal as the total stored energy of the two arms is regulated by the energy regulator.

The overlap operation of the AAC is modeled similarly to the MMC operation for energy regulation using the circulating current. Average stored energy difference between two arms of an MMC phase-leg caused by unbalanced arm impedances is balanced injecting a common mode fundamental component to the circulating current [11]. Unlike the continuous circulating current of the MMC, the circulating current of AAC is limited to the overlap period. Therefore during the overlap period, a common mode current component can be introduced to the circulating current, instead of a fundamental component, to balance the energy difference between the arms. This can be achieved by scaling the differential voltages across the upper and lower arm inductances and generating a common mode voltage component [9].

Unbalanced SM capacitances cause SM capacitor voltage ripple variation so the energy variation do not influence the average stored energy of the arms. This leads to unbalanced losses distribution among the SMs, and improved SM capacitor sorting/balancing algorithms are used to balance the losses [12].

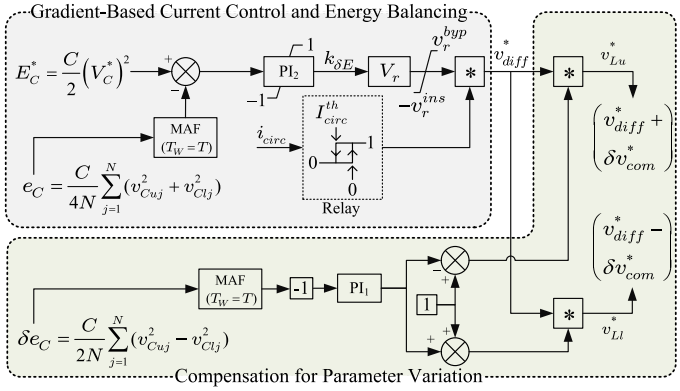

Fig. 1. Proposed compensation method.

B. Proposed Compensation Method

The proposed compensation method for energy balancing under parameter variation (see Fig. 1) is developed as an extension of the gradient-based current control method [7]. The gradient-based current controller provides the differential voltage reference ($v_{\rm diff}^*$) for both arms to regulate the stored energy within both arms. In the compensation stage, a common mode voltage component ($\delta v_{\rm com}^*$) which balances the energy difference between upper and lower arms is introduced to $v_{\rm diff}^*$.

A PI controller calculates the ratio ($\delta v_{\rm com}^*/v_{\rm diff}^*$) according to the energy deviation (δe_C), regulating δe_C to zero. Finally, the controller provides voltage references

$$v_{Lu}^* = v_{\rm diff}^* + \delta v_{\rm com}^*, \qquad \text{and} \tag{5}$$

$$v_{Ll}^* = v_{\rm diff}^* - \delta v_{\rm com}^* \tag{6}$$

for the arm inductances of the upper and lower arms. The transfer function of the proposed compensation loop for parameter variations can be written as follows:

$$\delta V_{\rm com}^*(s) = \left[\frac{(1-e^{-sT})(sk_p + k_i)\cdot V_{\rm diff}^*(s)}{s^2}\right]\delta E_C(s) \tag{7}$$

where k_p and k_i are the PI controller gains and $V_{\rm diff}^*(s)$ is the output of the gradient-based current controller.

Fig. 1, and (5) and (6) show that the proposed method modifies the voltage across each arm inductor. This includes the differential voltage that regulates the total stored energy within the phase-leg and the common-mode component (7) that balances the energy difference between the upper and lower arms. Hence, both energy regulation and energy balancing can be achieved by the proposed method. As the SM capacitance variations affect only the SM capacitor voltage ripples, the proposed compensation method is functional also under unbalanced SM capacitances.

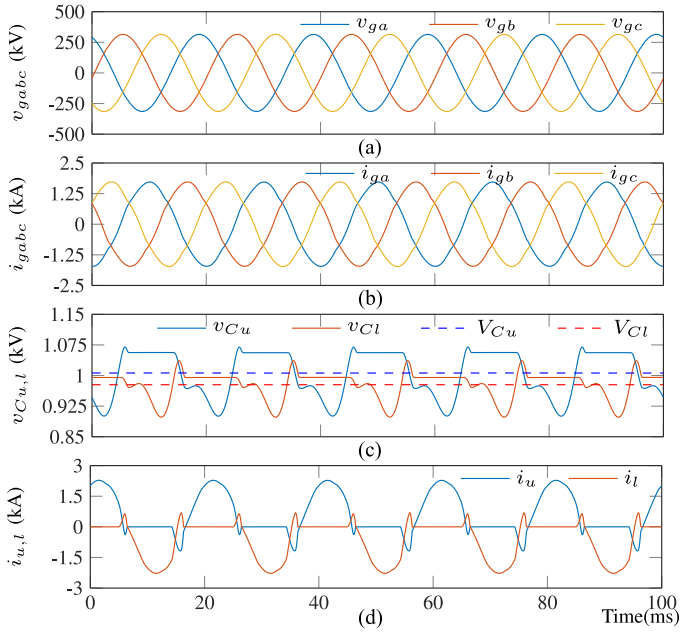

Fig. 2. Energy balancing capability of the AAC at $m_a = 1.15$ with $0.7L$ lower arm inductance of phase a. (a) Grid voltages. (b) Grid currents. (c) SM capacitor voltages of phase a. (d) Arm currents of phase a.

IV. Simulation Results

A. Real-Time HVDC Model

In order to demonstrate the energy balancing performance of the proposed compensation method under parameter variation, an AAC-HVDC system with 255 SMs per arm is used [10]. The model is derived from the CIGRE benchmark MMC-HVDC transmission system and developed in a real-time digital simulator. Readers are referred to [10] for a detailed description of the real-time model.

The AAC is operating at constant current and power factor. The power references are $P^* = p$ and $Q^* = 0.4p$, where apparent power $s = p\sqrt{1+(0.4)^2}$ is set proportional to the operating point m_a. Energy balancing performance of the proposed method is demonstrated compared to the conventional overlap period control method [5], and the gradient-based energy balancing method [7]. A typical ($m_a = 1.15$) and a lower ($m_a = 0.9$) operating point are considered under 30% reduction in the lower arm inductance and 10% reduction in the lower arm SM capacitances. In contrast to the MMC, the AAC requires smaller arm inductance [13]. Therefore, significant arm energy deviations are expected predominantly at considerably large arm inductor variations.

B. Energy Balancing Performance

Fig. 2 shows the energy balancing capability of the conventional overlap period control method at $m_a = 1.15$ and 70% of the nominal lower arm inductance of phase a. Fig. 2(c) and (d) shows the SM capacitor voltages and the arm currents of phase a. The SM capacitor voltages of both the upper and lower arms deviate from the reference. The arm currents within two consecutive overlap periods become unbalanced due to the common-mode current component caused by the arm inductance variations. The unbalanced arm currents within the overlap period lead to unequal charging/discharging of the SM capacitors and, hence, energy deviations 0.5% and −2.9% in upper and lower arms, respectively. The ac voltages and currents of Fig. 2(a) and (b) are not significantly affected by the energy deviation as the energy deviations are relatively small ($<|3|\%$) and the arm inductance size of the AAC is relatively small.

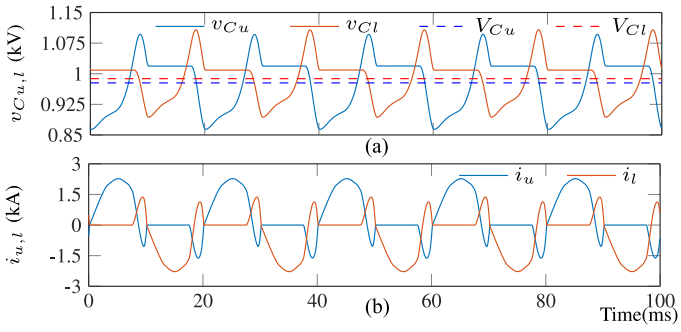

Fig. 3. Energy balancing capability of the AAC at $m_a = 0.9$ with $0.7L$ lower arm inductance of phase a. (a) SM capacitor voltages of phase a. (b) Arm currents of phase a.

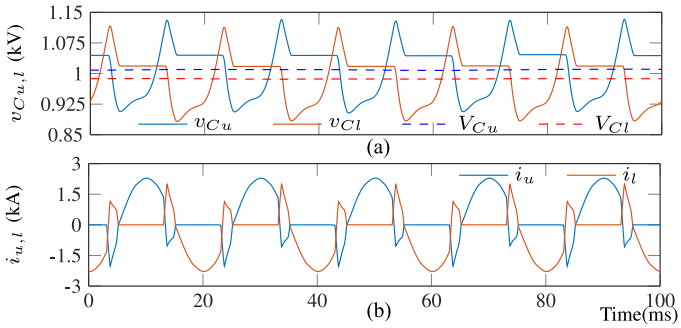

Fig. 4. Energy balancing capability of Gradient-based method [7] at $m_a = 0.9$ with $0.7L$ lower arm inductance of phase a. (a) SM capacitor voltages of phase a. (b) Arm currents of phase a.

Fig. 3 demonstrates the energy balancing capability of the AAC with conventional overlap period control method under the arm inductance variation similar to Fig. 2 at $m_a = 0.9$. The upper and lower arm SM capacitor voltages of Fig. 3(a) deviate from the reference due to the unbalanced arm currents of Fig. 3(b) within the overlap period. Resultant energy deviations of the upper and lower arms are −4.44% and −2.4%, respectively, and lead to a total stored energy deviation of −3.41%. Although the energy deviations are significant, the ac voltages and currents are similar to Fig. 2 and not significantly affected due to relatively low arm inductance requirement of the AAC.

The performance of the gradient-based energy balancing method under arm inductor variations is shown in Fig. 4. SM capacitor voltages of Fig. 4(a) deviate oppositely from the reference. As the gradient-based method is applied, the average energy of the phase-leg is regulated to the reference (total energy deviation is −0.35%), but the energy deviations of the upper and lower arms (1.84% and −2.55%, respectively) exist due to the arm inductance imbalance. Compared to the conventional overlap period control method of Fig. 3, the average energy deviation

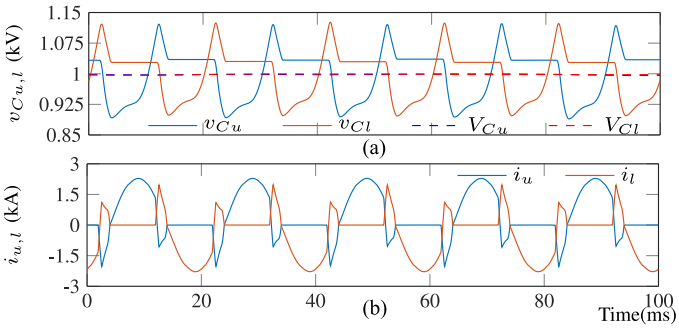

Fig. 5. Energy balancing capability of the proposed method at $m_a = 0.9$ with $0.7L$ lower arm inductance of phase a. (a) SM capacitor voltages of phase a. (b) Arm currents of phase a.

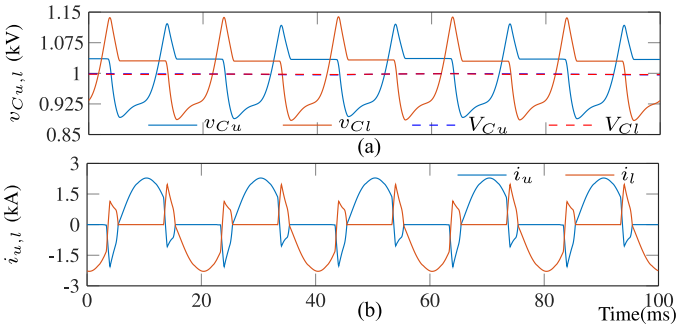

Fig. 6. Energy balancing capability of the proposed method at $m_a = 0.9$ with $0.7L$ lower arm inductance and $0.9C$ lower arm SM capacitances of phase a. (a) SM capacitor voltages of phase a. (b) Arm currents of phase a.

of the phase-leg reduces approximately by $|3|\%$. Accordingly, the arm current imbalance among consecutive overlap periods also reduces as seen in Fig. 4(b). Therefore, the gradient-based method regulates the average energy of the phase-leg and assists reducing the arm current imbalance, but additional control is required to further reduce arm energy deviations.

The proposed method of Fig. 1 is applied and Fig. 5 shows its energy balancing performance under arm inductance imbalances. The upper and lower arm SM capacitor voltages of Fig. 5(a) are regulated to the reference. The total arm energy, upper arm energy, and lower arm energy deviations are -0.35%, -0.36%, and -0.34%, respectively. Arm currents of Fig. 5(b) are balanced due to the circulating current control performed by the proposed compensation method.

The performance of the proposed method is further investigated under both arm inductance and SM capacitance variations. Although unlikely in practice, all the SM capacitances of the lower arm are reduced by 10% of the nominal value to demonstrate the performance of the proposed method under extreme unbalanced conditions. Fig. 6(a) demonstrates the energy balancing capability of the proposed under both arm inductance and SM capacitance variations. The SM capacitor voltage ripple increases due to the 10% capacitance reduction while the arm currents [see Fig. 6(b)] and ac side voltages, currents, and arm currents are not affected by the proposed method.

Fig. 7 evaluates the energy balancing performance of conventional overlap period control, gradient-based energy balancing, and proposed method under arm inductance variations, considering a typical range of AAC operating points

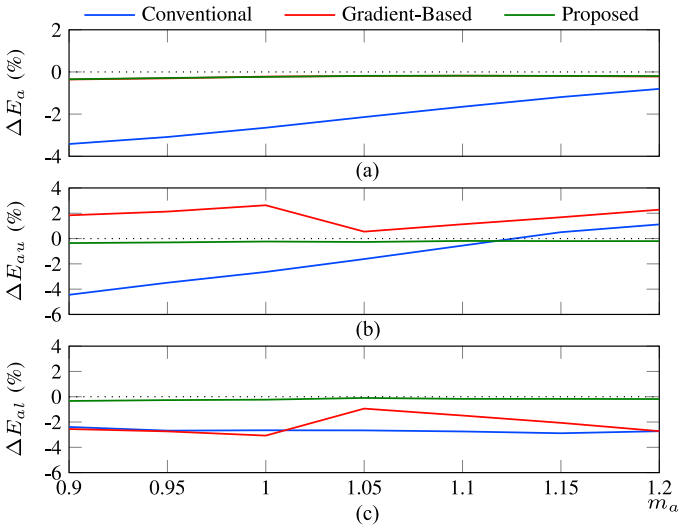

Fig. 7. Energy deviations of phase a with $0.7L$ lower arm inductance. (a) Average energy deviation of the phase-leg. (b) Average energy deviation of the upper arm. (c) Average energy deviation of the lower arm.

($0.9 \leq m_a \leq 1.2$). Fig. 7(a)–(c) shows that the average stored energy deviation of the phase-leg (ΔE_a) is significant and arm energy deviations (ΔE_{au} and ΔE_{al}) are asymmetric under the conventional overlap period control method. The gradient-based energy balancing method regulates the average stored energy ($\Delta E_a \approx 0$) and leads to fairly symmetric energy deviations ($\Delta E_{au} \approx -\Delta E_{al}$) between the upper and lower arms. Finally, the proposed method regulates the average stored energy ($\Delta E_a \approx 0$) of the phase-leg and reduces the energy deviations ($\Delta E_{au} \approx 0$ and $\Delta E_{al} \approx 0$) of the upper and lower arms, demonstrating improved energy balancing capability under parameter variations.

V. Conclusion

Energy balancing is challenging at the nonsweet-spot operation of the AAC. This paper has studied the energy balancing capabilities of overlap period-based circulating current control under component parameter variations and proposed a compensation method for the gradient-based circulating current control in order to balance the energy under arm inductance and SM capacitance variations of the AAC. The proposed method scales the differential voltage depending on arm energy deviation, imposing a common-mode current component in the circulating current that reduces the arm energy imbalance. The results based on a real-time AAC-HVDC transmission system model demonstrate that the proposed method delivers improved energy balancing performance for the AAC even at lower operating points under different AAC parameter variations and is an important component in the operation of the AAC.

References

[1] H. Akagi, "Multilevel converters: Fundamental circuits and systems," *Proc. IEEE*, vol. 105, no. 11, pp. 2048–2065, Nov. 2017.

[2] M. Barnes, D. V. Hertem, S. P. Teeuwsen, and M. Callavik, "HVDC systems in smart grids," *Proc. IEEE*, vol. 105, no. 11, pp. 2082–2098, Nov. 2017.

[3] M. M. C. Merlin *et al.*, "The AAC: A new hybrid multilevel converter with dc-fault blocking capability," *IEEE Trans. Power Del.*, vol. 29, no. 1, pp. 310–317, Oct. 2014.
[4] M. M. C. Merlin and T. C. Green, "Cell capacitor sizing in multilevel converters: cases of the MMC and AAC," *IET Power Electron.*, vol. 8, no. 3, pp. 350–360, Mar. 2015.
[5] E. Farr, R. Feldman, A. Watson, J. Clare, and P. Wheeler, "A sub-module capacitor voltage balancing scheme for the AAC," in *Proc. 15th Eur. Conf. Power Electron. Appl.*, 2013, pp. 1–10.
[6] H. R. Wickramasinghe, G. Konstantinou, J. Pou, and V. G. Agelidis, "Asymmetric overlap and hysteresis current control of zero-current switched AAC," in *Proc. 42nd Annu. Conf. IEEE Ind. Electron. Soc.*, Oct. 2016, pp. 2526–2531.
[7] H. R. Wickramasinghe, G. Konstantinou, and J. Pou, "Gradient-based energy balancing and current control for alternate arm converters," *IEEE Trans. Power Del.*, vol. 33, no. 3, pp. 1459–1468, Jun. 2018.
[8] M. Mehrasa, E. Pouresmaeil, M. F. Akorede, S. Zabihi, and J. P. S. Catalo, "Function-based modulation control for MMCs under varying loading and parameters conditions," *IET Gener., Transmiss. Distrib.*, vol. 11, no. 13, pp. 3222–3230, Oct. 2017.
[9] Y. Zhou, D. Jiang, J. Guo, P. Hu, and Y. Liang, "Analysis and control of MMCs under unbalanced conditions," *IEEE Trans. Power Del.*, vol. 28, no. 4, pp. 1986–1995, Oct. 2013.
[10] H. R. Wickramasinghe, G. Konstantinou, Z. Li, and J. Pou, "Alternate arm converters-based HVDC model compatible with the CIGRE B4 DC grid test system," *IEEE Trans. Power Del.*, p. 1, 2018, doi: 10.1109/TPWRD.2018.2850933
[11] J. Pou, S. Ceballos, G. Konstantinou, V. G. Agelidis, R. Picas, and J. Zaragoza, "Circulating current injection methods based on instantaneous information for the MMC," *IEEE Trans. Ind. Electron.*, vol. 62, no. 2, pp. 777–788, Feb. 2015.
[12] G. Konstantinou, H. R. Wickramasinghe, S. Ceballos, and J. Pou, "Submodule voltage balancing and loss equalisation in alternate arm converters based on virtual voltages," in *Proc. ECCE Asia*, Niigata, Japan, 2018, pp. 1–6.
[13] M. M. C. Merlin *et al.*, "The extended overlap AAC: A VSC with dc fault ride-through capability and a compact design," *IEEE Trans. Power Electron.*, vol. 33, no. 5, pp. 3898–3910, May 2018.